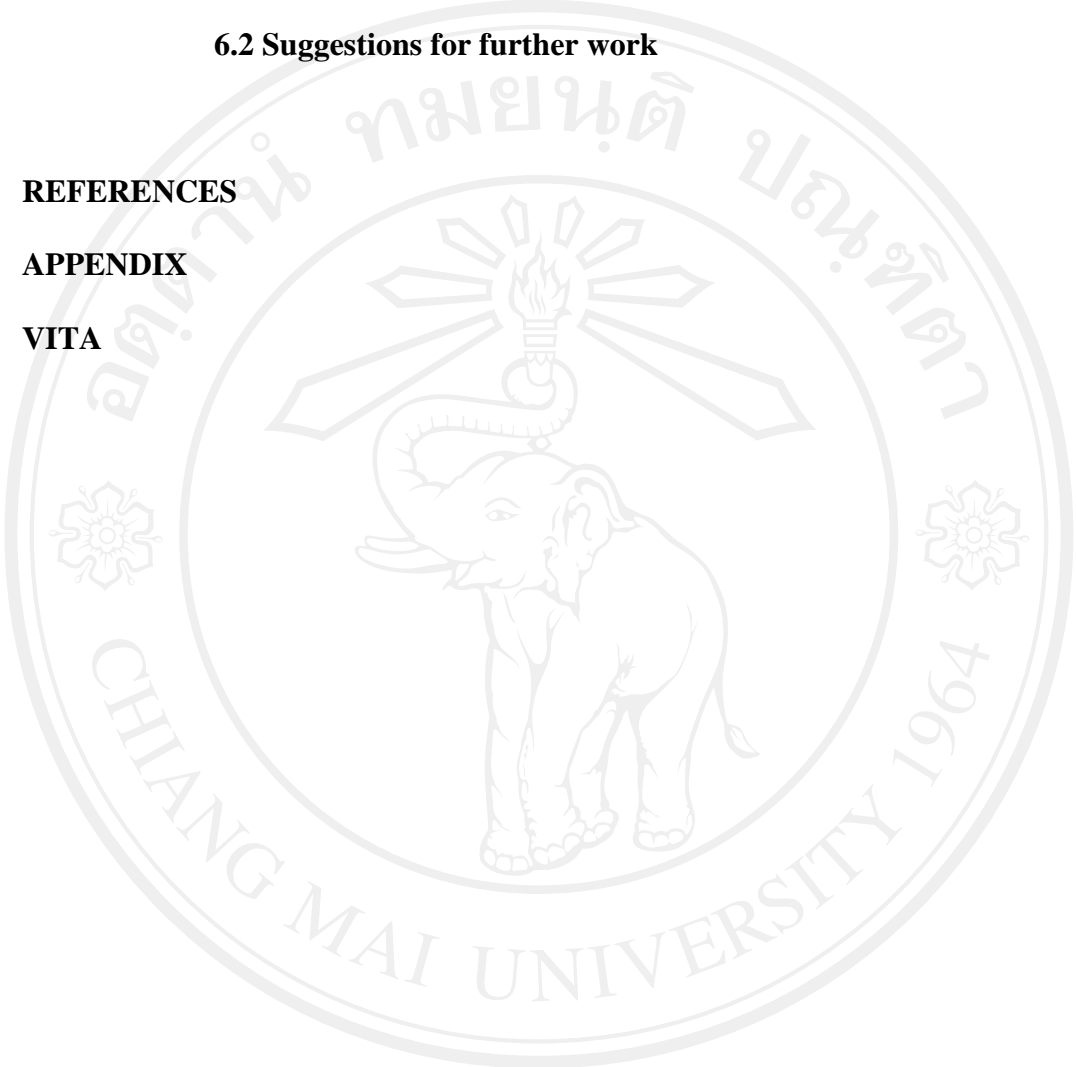


	Page
2.1.2 Applications	7
2.1.3 Lithium niobate (LiNbO ₃)	9
2.2 Glass	12
2.2.1 Theory of glass	14
2.2.2 Raw materials for glass melting	17
2.2.3 Atomic hypothesis of glass formation	21
2.2.4 Nucleation and crystallization	22
2.2.5 Controlled crystallization	28
2.3 Glass-ceramics	29
2.3.1 History	29
2.3.2 Theory of glass-ceramics	30
2.3.3 Applications	31
2.4 Literature Review	32
2.4.1 Lithium-based glasses and glass-ceramics	33
2.4.1.1 Crystallization and glass formation in 50Li ₂ O · 50Nb ₂ O ₅ and 25Li ₂ O · 25Nb ₂ O ₅ · 50SiO ₂	33
2.4.1.2 Lithium niobate ferroelectric material obtained by glass crystallization	35
2.4.1.3 Evolution of ferroelectric LiNbO ₃ phase in a reactive glass matrix (LiBO ₂ · Nb ₂ O ₅)	37

	Page
2.4.2 Others ferroelectric-based glasses and glass-ceramics	39
2.4.2.1 Crystallization of $\text{Bi}_4\text{Ti}_3\text{O}_{12}$ from glasses in the system $\text{Bi}_2\text{O}_3/\text{TiO}_2/\text{B}_2\text{O}_3$	39
2.4.2.2 Crystallization of $\text{Bi}_3\text{TiNbO}_9$ from glasses in the system $\text{Bi}_2\text{O}_3/\text{TiO}_2/\text{Nb}_2\text{O}_5/\text{B}_2\text{O}_3/\text{SiO}_2$	40
2.4.2.3 Crystallization of ferroelectric bismuth vanadate in $\text{Bi}_2\text{O}_3 \cdot \text{V}_2\text{O}_5 \cdot \text{SrB}_4\text{O}_7$ glasses	40
2.4.2.4 $\text{BiO}_{1.5} \cdot \text{BO}_{1.5} \cdot \text{GeO}_2$ glass system and crystallization of $\text{Bi}_4\text{Ge}_3\text{O}_{12}$ phase	41
2.4.2.5 Nanocrystallization of $\text{SrBi}_2\text{Nb}_2\text{O}_9$ from glasses in the system $\text{Li}_2\text{B}_4\text{O}_7 \cdot \text{SrO} \cdot \text{Bi}_2\text{O}_3 \cdot \text{Nb}_2\text{O}_5$	43
CHAPTER 3 EXPERIMENTAL PROCEDURE	45
3.1 Samples preparation	45
3.1.1 LiNbO_3 powder	45
3.1.2 Glass samples	47
3.1.3 Glass-ceramic samples	51
3.2 Glass and glass-ceramic samples characterization	52
3.2.1 Thermal analysis	52
3.2.2 Densification analysis	55

	Page
4.5.1 Surface morphology of glass samples	86
4.5.2 Cross-sectional morphology of glass and glass-ceramic samples	91
4.6 Optical properties	98
4.6.1 Transmittance (%)	98
4.6.2 Refractive index	102
4.7 Electrical property	103
CHAPTER 5 RESULTS AND DISCUSSION (PART II): LiNbO₃ · SiO₂ · Al₂O₃ GLASS SYSTEM	109
5.1 Appearance	109
5.2 Thermal behavior determination	111
5.3 Structural information	112
5.3.1 X-ray diffractometry	112
5.3.2 Raman spectroscopy	116
5.4 Microstructure observation	117
5.5 Electrical property	119
CHAPTER 6 CONCLUSIONS AND SUGGESTIONS FOR FUTURE WORK	122
6.1 Conclusions	122
6.1.1 LiNbO ₃ · SiO ₂ glass and glass-ceramic system	122

	Page
6.1.2 $\text{LiNbO}_3 \cdot \text{SiO}_2 \cdot \text{Al}_2\text{O}_3$ glass system	124
6.2 Suggestions for further work	124
REFERENCES	126
APPENDIX	137
VITA	153



ลิขสิทธิ์มหาวิทยาลัยเชียงใหม่
Copyright© by Chiang Mai University
All rights reserved

LIST OF TABLES

Table	Page
2.1 Basic properties of lithium niobate.	10
2.2 Composition and characteristics of some common commercial glasses.	13
2.3 Heat treatment conditions, visual appearance and phase compositions of the sample L-4.	36
3.1 Specifications of the raw materials used for preparation LiNbO_3 powder and glass samples.	46
3.2 Chemical compositions of the prepared glass samples.	50
3.3 The density of the fluid (distilled water) at various temperatures.	56
4.1 Typical DTA curves obtained for the powder of the glass samples corresponding to the compositions.	75
4.2 Compositional variations of densities measured on the glass and glass-ceramic samples at different heat treatment temperatures.	77
4.3 Compositional variations of densities measured on the glass and glass-ceramic samples at different heating times.	79
4.4 Mean crystallite sizes (calculated by Scherrer equation) of glass-ceramic samples at 600, 650, 700 and 975 °C for 1 h with 20, 25, 30 and 35 mol% SiO_2 .	84

Table	Page
4.5 Relative permittivity (ϵ_r) of glass and glass-ceramic samples at 600, 650, 700 and 975 °C for 1 h with 25 mol% SiO ₂ .	106
4.6 Relative permittivity (ϵ_r) of glass and glass-ceramic samples at 600, 650, 700 and 975 °C for 1 h with 30 mol% SiO ₂ .	107
4.7 Relative permittivity (ϵ_r) of glass and glass-ceramic samples at 600, 650, 700 and 975 °C for 1 h with 35 mol% SiO ₂ .	108
5.1 Peak intensity and mean crystallite sizes (calculated by Scherrer equation) of quenched samples with 15, 25, 35, 45 and 55 mol% SiO ₂ .	115
5.2 Relative permittivity (ϵ_r) of quenched samples with various compositions.	121
6.1 Comparison relative permittivity value at room temperature and 1 kHz of glass samples in this research with others nearly research.	123

LIST OF FIGURES

Figure		Page
2.1	Polarization of (a) dielectric, (b) paraelectric and (c) ferroelectric.	6
2.2	Crystal structure of LiNbO_3 showing the octahedral oxygen coordination spheres of niobium.	11
2.3	Comparison of glass structure: (a) random amorphous structure and (b) ordered crystalline structure.	12
2.4	Effect of temperature on the enthalpy of a glass forming melts.	16
2.5	Diagram of nucleation and crystallization.	23
2.6	Rates of homogeneous nucleation and crystal growth in a viscous liquid.	27
2.7	Schematic diagram of idealized heat treatment; x: heating rate, y: heat treatment temperature and z: dwell time.	28
2.8	Micrographs of surface morphologies of $50\text{Li}_2\text{O} \cdot 50\text{Nb}_2\text{O}_5$ glass-ceramics: (a) one-side quenching and (b) two-side quenching.	33
2.9	XRD patterns of $50\text{Li}_2\text{O} \cdot 50\text{Nb}_2\text{O}_5$ glass-ceramics: (a) one-side quenching and (b) two-side quenching.	34
2.10	XRD patterns of $25\text{Li}_2\text{O} \cdot 25\text{Nb}_2\text{O}_5 \cdot 50\text{SiO}_2$ glass-ceramics: (a) as-quenching and (b) heat treatment at $800\text{ }^\circ\text{C}$ for 30 min.	35
2.11	XRD patterns of the as-quenched ((a)-(b)) and the samples heat-treated at $500\text{ }^\circ\text{C}$ for 3 h ((c)-(f)).	38

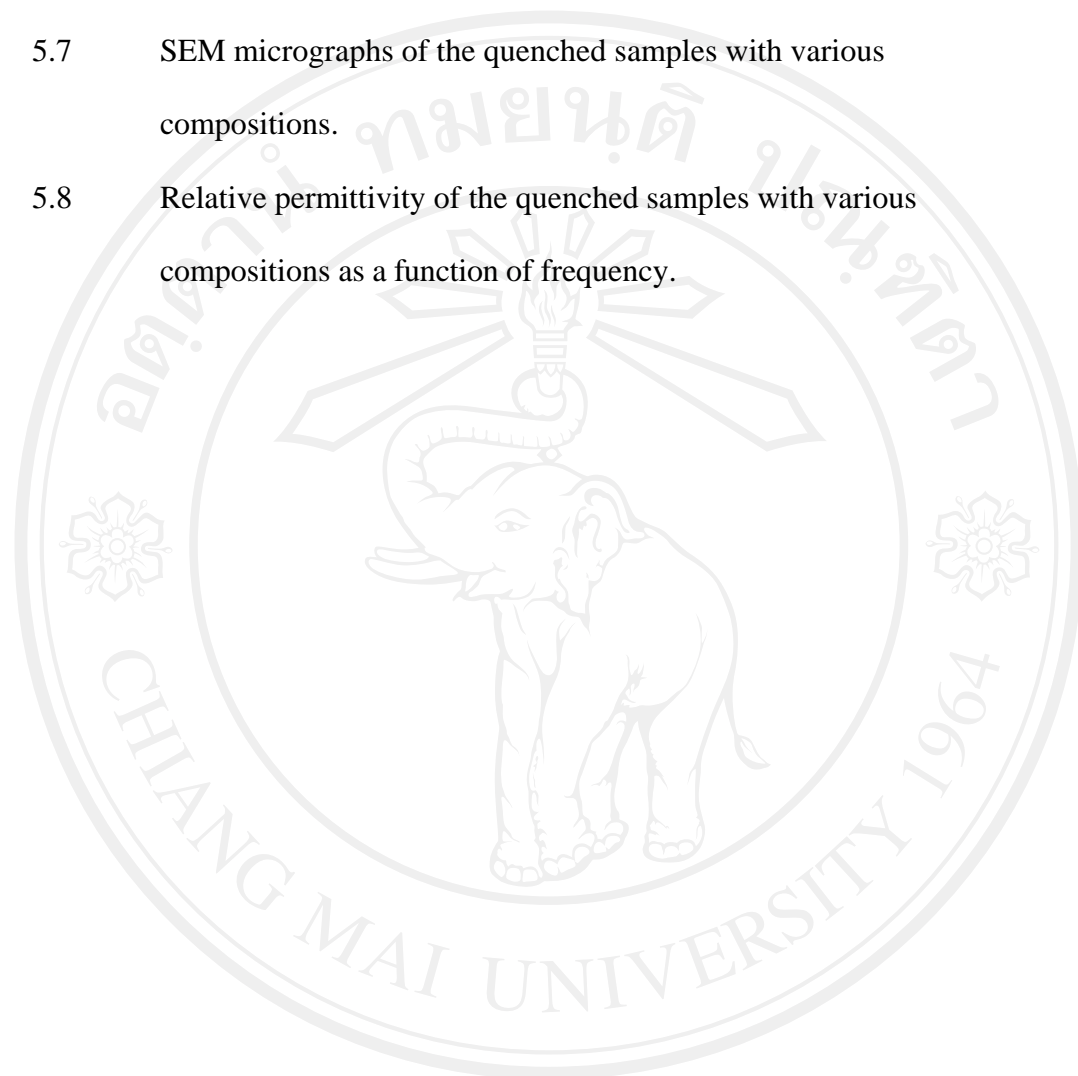
Figure	Page
2.12 SEM records of the samples heat-treated at different temperatures: (a) 475 °C, (b) 500 °C, (c) 600 °C and it shows voids/micro crack formation and (d) 650 °C.	39
2.13 XRD patterns of the as-quenched samples ((a)-(c)) and the glass- ceramic samples ((d)-(f)).	41
2.14 XRD pattern of the glass sample (45BiO _{1.5} · 40BO _{1.5} · 15GeO ₂).	42
2.15 SEM microphotographs of crystallized sample (45BiO _{1.5} · 40BO _{1.5} · 15GeO ₂): (a) prismatic crystals are Bi ₆ B ₁₀ O ₂₄ and (b) pyramid- shaped crystals are Bi ₄ Ge ₃ O ₁₂ .	42
2.16 XRD patterns of 40(Li ₂ B ₄ O ₇) · 60(SrO · Bi ₂ O ₃ · Nb ₂ O ₅) samples: (a) as-quenched, heat-treated at (b) 450 °C, (c) 500 °C, (d) 550 °C and (e) 625 °C and slow scan is shown in the inset.	44
3.1 Melting electric furnace.	48
3.2 Pouring melting glass onto a brass block.	48
3.3 Glass sample.	49
3.4 Annealing electric furnace.	49
3.5 Transparent glass sample.	51
3.6 Thermogravimetric analyzer.	53
3.7 Differential thermal analyzer.	54
3.8 Balance with density equipment.	58
3.9 Pycnometer.	58
3.10 X-ray diffractometer.	59

Figure	Page
3.11 Raman spectrometer.	61
3.12 Scanning electron microscope, equipped with EDX analyzer.	62
3.13 Transmission electron microscope.	62
3.14 UV-Vis-NIR spectrophotometer.	65
3.15 The absorbance spectrum of nickel, copper and nickel coin.	65
3.16 Impedance spectroscopy (Kronach).	68
3.17 Roughly polished sample (left side) and after using gold-contacting paste (right side): (a) top view and (b) side view.	68
3.18 Impedance spectroscopy (Hewlett).	69
4.1 Glass samples with various compositions.	71
4.2 Transparency of glasses and glass-ceramics of four compositions.	72
4.3 DTA profiles of the glass samples with various compositions.	76
4.4 The glass transition temperature (T_g) and the temperature of the first crystallization peak (T_{Cr1}) as a function of mol% SiO_2 (error in the temperatures ± 10 K).	76
4.5 Densities of the glass and glass-ceramic samples at different heat treatment temperatures.	78
4.6 Densities of the glass and glass-ceramic samples at different heating times.	79
4.7 XRD patterns of glass samples with various compositions (red arrow indicates cristobalite phase).	81
4.8 XRD patterns of glass and glass-ceramic samples with 20 mol% SiO_2 at different heat treatment temperatures.	82

Figure	Page
4.9 XRD patterns of glass and glass-ceramic samples with 25 mol% SiO ₂ at different heat treatment temperatures.	83
4.10 XRD patterns of glass and glass-ceramic samples with 30 mol% SiO ₂ at different heat treatment temperatures.	83
4.11 XRD patterns of glass and glass-ceramic samples with 35 mol% SiO ₂ at different heat treatment temperatures.	84
4.12 XRD patterns of glass and glass-ceramic samples with 35 mol% SiO ₂ at different heating times.	85
4.13 SEM and TEM micrographs of the glass sample with 20 mol% SiO ₂ .	87
4.14 SEM and TEM micrographs of the glass sample with 25 mol% SiO ₂ .	87
4.15 SEM and TEM micrographs of the glass sample with 30 mol% SiO ₂ .	88
4.16 SEM and TEM micrographs of the glass sample with 35 mol% SiO ₂ .	88
4.17 SEM and TEM micrographs of the glass sample with 40 mol% SiO ₂ .	89
4.18 SEM and TEM micrographs of the glass sample with 50 mol% SiO ₂ .	89
4.19 SEM micrographs (BSE detector) of heat-treated samples at 700 °C for 1 h with 40, 45, 50 and 60 mol% SiO ₂	90
4.20 SEM micrographs of the glass and glass-ceramic samples with 20 mol% SiO ₂ .	93
4.21 SEM micrographs of the glass and glass-ceramic samples with 25 mol% SiO ₂ .	94
4.22 SEM micrographs of the glass and glass-ceramic samples with 30 mol% SiO ₂ .	95

Figure	Page
4.23 SEM micrographs of the glass and glass-ceramic samples with 35 mol% SiO ₂ .	96
4.24 The optical transmission spectra and images of glass and glass-ceramic samples with 25 mol% SiO ₂ (minor scale = 1 mm).	99
4.25 The optical transmission spectra and images of glass and glass-ceramic samples with 30 mol% SiO ₂ (minor scale = 1 mm).	100
4.26 The optical transmission spectra and images of glass and glass-ceramic samples with 35 mol% SiO ₂ (minor scale = 1 mm).	101
4.27 Refractive index of glass samples.	102
4.28 Variation of relative permittivity (ϵ_r) as a function of frequency with 25 mol% SiO ₂ .	104
4.29 Variation of relative permittivity (ϵ_r) as a function of frequency with 30 mol% SiO ₂ .	104
4.30 Variation of relative permittivity (ϵ_r) as a function of frequency with 35 mol% SiO ₂ .	105
4.31 Relative permittivity (ϵ_r) of glass and glass-ceramic samples with 25, 30 and 35 mol% SiO ₂ as heat-treated at 700 °C for 1 h.	105
5.1 Quenched samples with various compositions.	110
5.2 DTA profiles of the quenched samples with 15 mol% SiO ₂ .	111
5.3 XRD patterns of quenched samples with various compositions.	113
5.4 The relationship between 012 peak intensity and SiO ₂ content.	114
5.5 The relationship between the mean crystallite sizes and SiO ₂ content.	114

Figure		Page
5.6	Raman spectra of the quenched samples.	116
5.7	SEM micrographs of the quenched samples with various compositions.	118
5.8	Relative permittivity of the quenched samples with various compositions as a function of frequency.	120



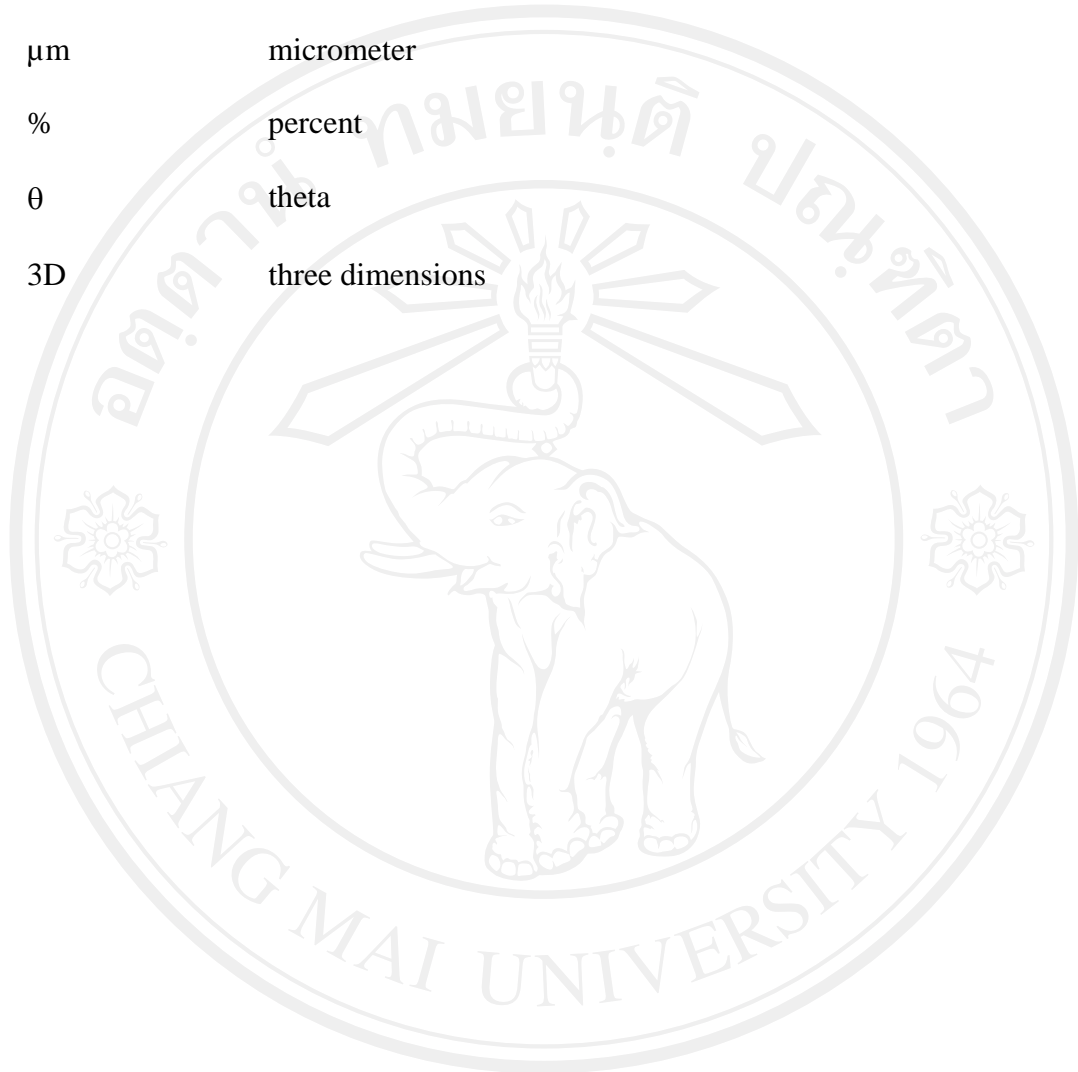
ลิขสิทธิ์มหาวิทยาลัยเชียงใหม่
Copyright© by Chiang Mai University
All rights reserved

ABBREVIATIONS AND SYMBOLS

ASTM.	American society for testing materials
a.u.	arbitrary unit
BSE	back scattered electron
DSC	differential scanning calorimetry
DTA	differential thermal analysis
EDX	energy dispersive X-ray spectrometry
eV	electron volt
F/m	farad per meter
FWHM	the full width at half maximum
g	gram
g/cm ³	gram per cubic centimeter
h	hour
HT	heat treatment
JCPDS	Joint Committee for Powder Diffraction Standards
K	Kelvin
kHz	kilohertz
K/min	Kelvin per minute
kV	kilovolt
mA	milliampere
mg	milligram

MHz	megahertz
min	minute
mm	millimeter
mol%	percent molar
mW	milliwatt
NLO	nonlinear optical coefficients
nm	nanometer
OD	optical density
pm/V	picometer per volt
SEM	scanning electron microscopy
TEM	transmission electron microscopy
TGA	thermogravimetric analysis
T_c	the Curie temperature
T_{Cr}	crystallization temperature
T_F	fictive temperature
T_g	glass transition temperature
T_m	melting temperature
T_n	nucleation temperature
UV-Vis-NIR	ultraviolet-visible-near infrared spectrophotometry
V	volt
wt%	percent weight
XRD	X-ray Diffraction
Å	angstrom

°C	degree Celsius
°C/min	degree Celsius per minute
μm	micrometer
%	percent
θ	theta
3D	three dimensions



ลิขสิทธิ์มหาวิทยาลัยเชียงใหม่
Copyright© by Chiang Mai University
All rights reserved